

Conformational Analysis, Infrared, and Fluorescence Spectra of 1-Phenyl-1,2-propandione 1-oxime and Related Tautomers: Experimental and Theoretical Study

Ahmad R. Bekhradnia¹ and Sattar Arshadi^{2,*}

¹ Department of Chemistry and Pharmaceutical Science Research Center, Mazandaran University of Medical Sciences, Sari, Iran

² Department of Chemistry, University of Payame Noor, Behshahr, Iran

Received December 12, 2006; accepted January 24, 2007; published online May 31, 2007

© Springer-Verlag 2007

Summary. Conformational analysis and frequency calculation were achieved for 1-phenyl-1,2-propandione 1-oxime and its four tautomers: 1-nitroso-1-phenyl-1-propen-2-ol, 1-nitroso-1-phenyl-2-propanone, 2-hydroxy-1-phenyl-propenone oxime, and 3-nitroso-3-phenyl-propen-2-ol. Calculations were carried out at the *Hartree–Fock* (HF), Density Functional Theory (B3LYP), and the second-order *Møller–Plesset* perturbation (MP2) levels of theory using 6-31G* and 6-311G** basis sets. Five conformers with no imaginary vibrational frequency were obtained by free rotations around three single bonds of 1-phenyl-1,2-propandione-1-oxime: *Ph*–C(NOH)C(O)CH₃, *Ph*C(NOH)–C(O)CH₃, and *Ph*C(N–OH)C(O)CH₃. Similarly, eight structures with no imaginary vibrational frequency were encountered upon rotations around three single bonds of 1-nitroso-1-phenyl-1-propen-2-ol: *Ph*–C(NO)C(OH)CH₃, *Ph*C(N–O)C(OH)CH₃, and *Ph*C(NO)C(–OH)CH₃. In the same manner, six minima were found through rotations around three single bonds of 1-nitroso-1-phenyl-2-propanone: *Ph*–CH(NO)C(O)CH₃, *Ph*CH(–NO)C(O)CH₃, and *Ph*CH(NO)–C(O)CH₃. Also, two minima were found through rotations around four single bonds of 2-hydroxy-1-phenyl-propenone oxime: *Ph*–C(NOH)C(OH)CH₂, *Ph*C(N–OH)C(OH)CH₂, *Ph*C(NOH)–C(OH)CH₂, and *Ph*–C(NOH)C(–OH)CH₂. Finally, two minima were found through rotations around four single bonds of 3-nitroso-3-phenyl-propen-2-ol: *Ph*–CH(NO)C(OH)CH₂, *Ph*CH(–NO)C(OH)CH₂, *Ph*CH(NO)–C(OH)CH₂, and *Ph*CH(NO)C(–OH)CH₂. Interconversions within the above sets of conformers were probed through scanning (one and/or two dimensional), and/or QST3 techniques. The order of the stability of global minima encountered was: 1,2-propandione-1-oxime > 1-nitroso-1-phenyl-2-propanone >

1-nitroso-1-phenyl-1-propen-2-ol > 2-hydroxy-1-phenyl-propenone oxime > 3-nitroso-3-phenyl-propen-2-ol. Hydrogen bonding appears significant in tautomers of 1-nitroso-1-phenyl-1-propen-2-ol and 2-hydroxy-1-phenyl-propenone oxime. The CIS simulated λ_{\max} for the first excited singlet state (S₁) of 1-phenyl-1,2-propandione 1-oxime is 300.4 nm, which was comparable to its experimental λ_{\max} of 312.0 nm. The calculated IR spectra of 1-phenyl-1,2-propandione 1-oxime and its tautomers were compared to the experimental spectra.

Keywords. *Ab initio*; DFT; Tautomerisation; MP2; 1-Phenyl-1,2-propandione 1-oxime.

Introduction

Oximes are found to be important substrates in stereoselective carbon–carbon bond forming reactions. They play an important role in the *Beckmann* rearrangement [1]. Since oximes have more than one conformer, the experimental and quantum chemical calculations for their conformational analysis are very interesting and have received a lot of attention among experimental and theoretical chemists [2]. For instance, the microwave spectrum of *n*-butyraldehyde oxime was observed in the frequency region 26.5–40 GHz, where four rotational conformers were found to exist in the gas phase; among these, two conformers belonged to the (*E*)-diastereomer and the other two to the (*Z*)-diastereomer. Also, the 2-nitrosophenol derivatives are in tautomeric equilibrium in

* Corresponding author. E-mail: sattar_arshadi@yahoo.com

solution [3, 4] with quinonemonooxime, but the nitroso form predominates [5]. *Buraway et al.* [3] have shown that in *n*-hexane, CCl_4 , CHCl_3 , Et_2O , benzene, ethanol, and water 2-nitrosophenol is present only as nitroso tautomer. In all solvents the compound studied exhibits the characteristic band of the nitroso group. In disagreement with the above experiment, *Jaffe's* [6] MO calculations have shown that the oxime form of 2-nitrosophenol should be more stable by 19.74 kJ/mol. *Ab initio* results for the total energies of both tautomers with intramolecular hydrogen bond indicate that the nitroso tautomer is more stable than the oxime tautomer by 43.06 and 23.81 kJ/mol at the *HF/6-31G* and *HF/6-31G** level [7]. In another incident, the tautomeric and conformational equilibrium of acenaphthenequinonemonooxime was studied by liquid and solid state NMR spectroscopy and *ab initio* calculations: it exists in the solid state as an oxime tautomer. However, in solution both the oxime and the

nitroso tautomeric forms are present. *Ab initio* 6-31G (d,p) calculations in agreement with the experimental data predict the oxime tautomer to be more stable [8]. Yet in another study, all the possible carbonyl-nitroso, enol-nitroso, and carbonyl-oxime conformations of glyoxalmonooxime and all the rotamers of the carbonyloxime tautomer of 1-methyl- and 2-methylglyoxalmonooximes have been theoretically investigated. The fully linear carbonyl-oxime conformer has been found to be the most favored one over the enol-nitroso and carbonyl-nitroso conformations [9].

Consequently, compounds capable of nitroso-oxime equilibria often show specific biological activities [10–11]. To carry out such biological functions, biomolecules must adopt definite conformational states. Again, this makes the study of oxime tautomeric conformations of prime importance and worth receiving attention [12–17]. In particular, the biologically active 1-phenyl-1,2-propanedione 1-oxime (**1**)

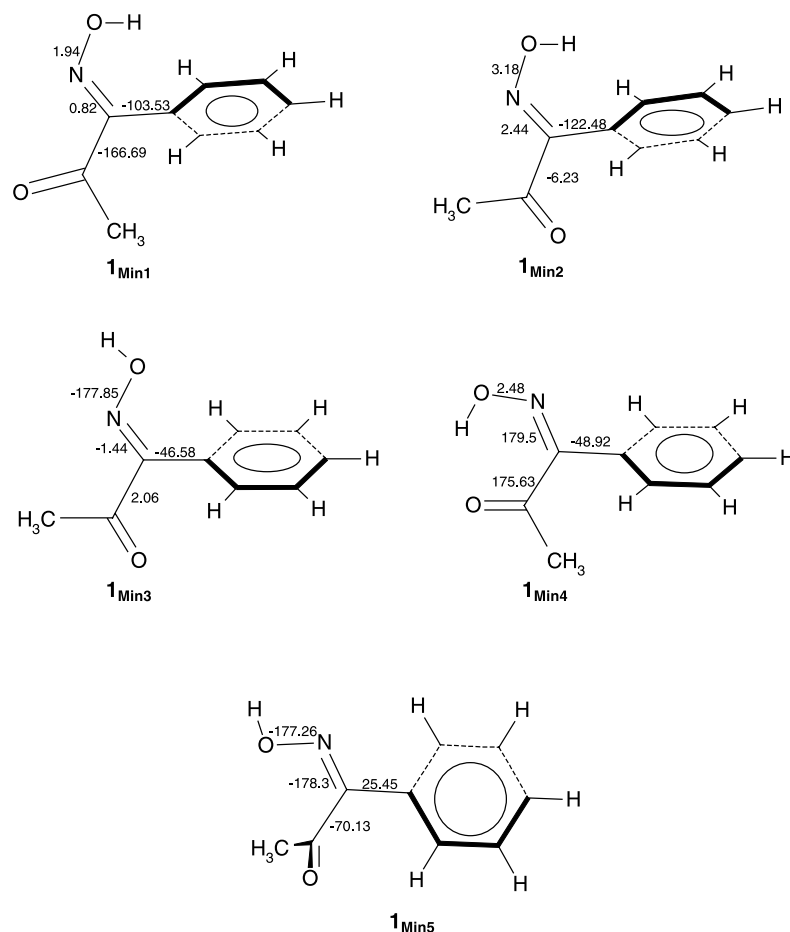


Fig. 1. The final optimized geometrical parameters (dihedral angles) of the five conformers of **1** obtained through DFT (*B3LYP/6-311G***) calculations

has electron donor atoms consisting of carbonyl oxygen and oxime nitrogen, which enable it to act as a mono- or bidentate ligand in metal complexes [18]. To date, no report has appeared on the conformational energy surface of **1** and its tautomers. In this paper, conformational energy surface, fluorescence, and IR spectral simulations are reported for **1** and its tautomers at the *Hartree-Fock* (*HF*), *DFT* (*B3LYP*), and second-order *Møller-Plesset* perturbation (*MP2*) levels of theory using 6-31G* and 6-311G** basis sets.

Results and Discussion

In this paper *HF*, *MP2*, and *DFT* methods with 6-31G** and 6-311G** basis sets were employed for investigating the tautomeric and conformational equilibria of 1-phenyl-1,2-propandione 1-oxime (**1**), 1-nitroso-1-phenyl-1-propen-2-ol (**2**), 1-nitroso-1-phenyl-2-propanone (**3**), 2-hydroxy-1-phenyl-propenone oxime (**4**), and 3-nitroso-3-phenyl-propen-2-ol (**5**) (Figs. 1–5). These were along with the calculated energy barriers separating the low energy conformers

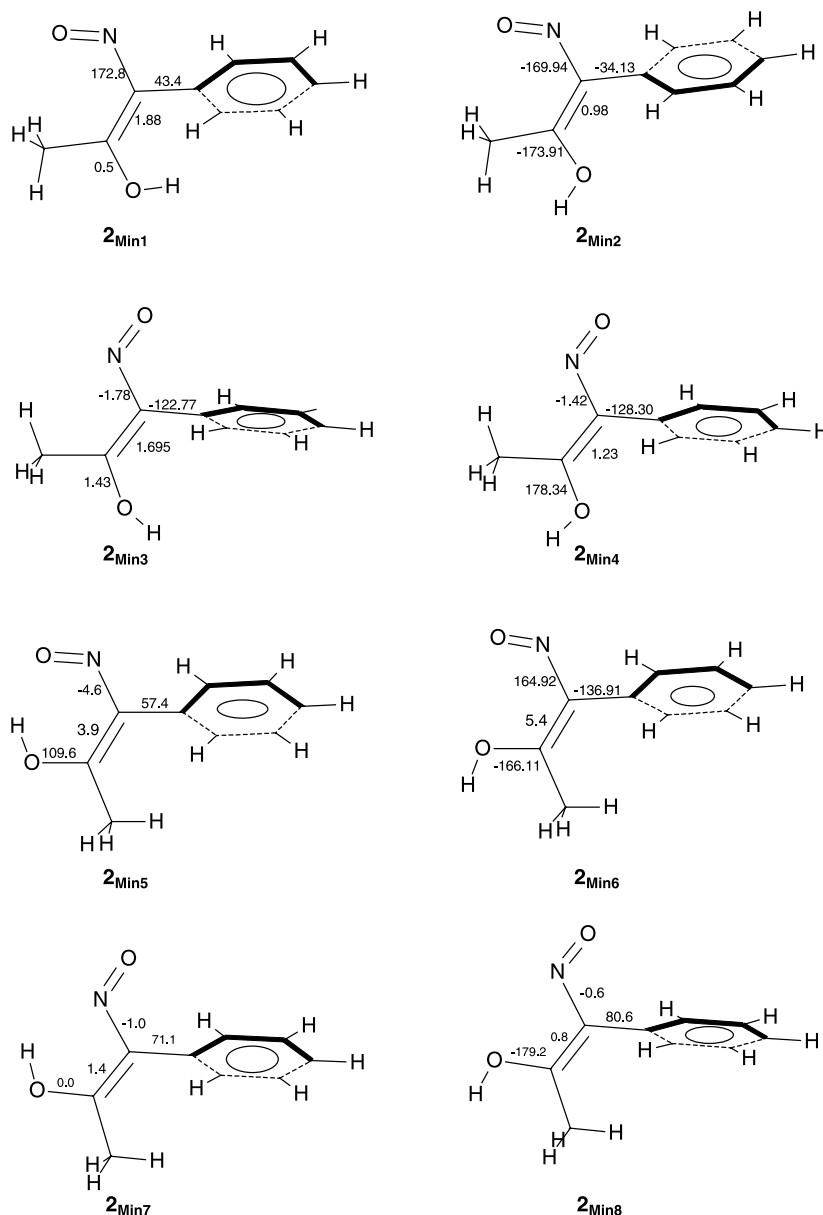


Fig. 2. The final optimized geometrical parameters (dihedral angles) of the eight conformers of **2** obtained by *DFT* (*B3LYP*/6-311G**) calculations

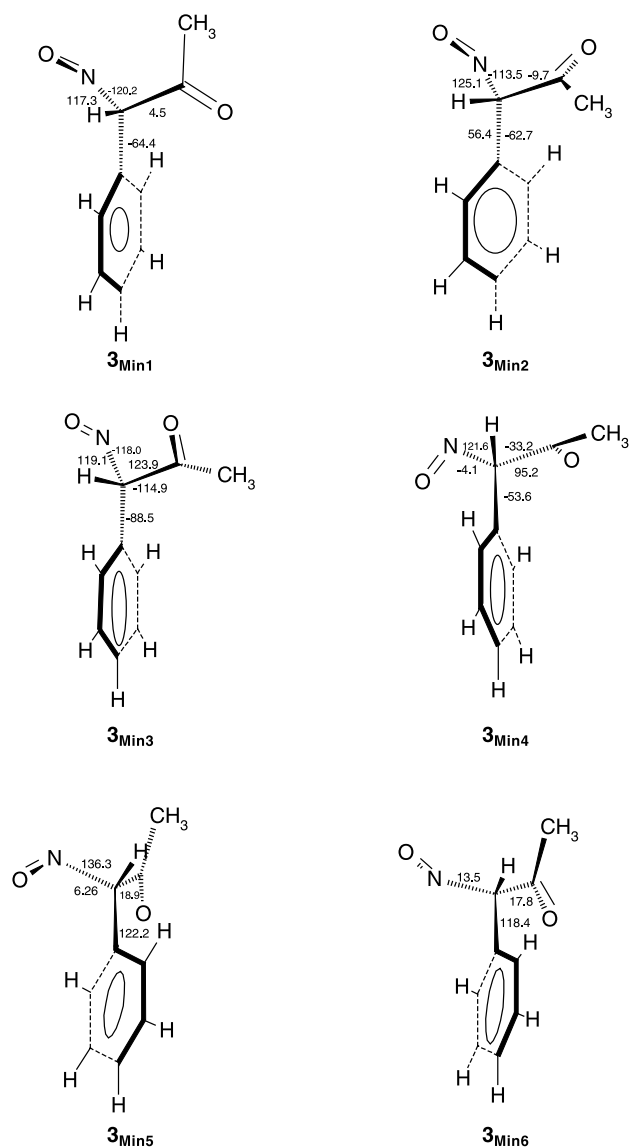


Fig. 3. The final optimized geometrical parameters (dihedral angles) of the six conformers of **3** obtained by DFT (*B3LYP/6-311G***) calculations

as well as the transition states in their inter-conversion pathways. In order to determine the barrier of internal rotations of different tautomers, we calculated the electronic energies of the molecules as a function of the angle of rotation about all single bonds.

The final optimized geometric structural parameters of conformers of **1**, **2**, **3**, **4**, and **5** were obtained by DFT (*B3LYP/6-311G***) calculations (Figs. 1–5). The results showed five rotamers (**1**_{Min1}, **1**_{Min2}, **1**_{Min3}, **1**_{Min4}, and **1**_{Min5}) to be important for conformational description of **1** (Fig. 1). Eight con-

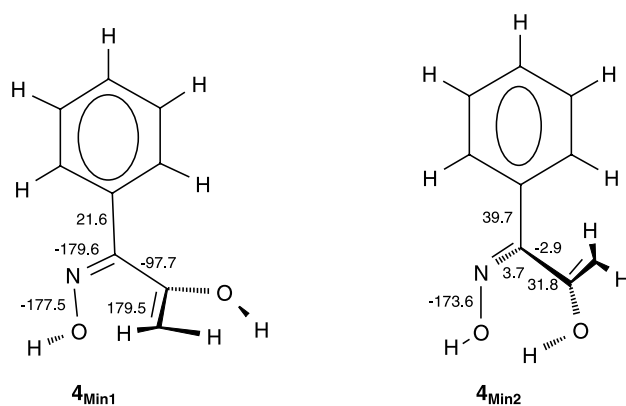


Fig. 4. The final optimized geometrical parameters (dihedral angles) of the two conformers of **4** obtained by DFT (*B3LYP/6-311G***) calculations

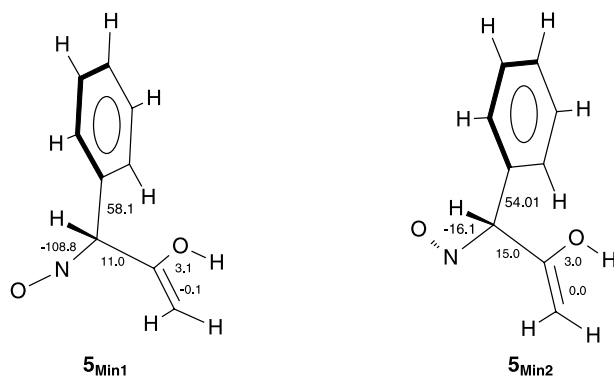


Fig. 5. The final optimized geometrical parameters (dihedral angles) of the two conformers of **5** obtained by DFT (*B3LYP/6-311G***) calculations

formers (**2**_{Min1}, **2**_{Min2}, **2**_{Min3}, **2**_{Min4}, **2**_{Min5}, **2**_{Min6}, **2**_{Min7}, and **2**_{Min8}) turned out to be significant for the conformational aspect of **2** (Fig. 2). Six conformers (**3**_{Min1}, **3**_{Min2}, **3**_{Min3}, **3**_{Min4}, **3**_{Min5}, and **3**_{Min6}) were essential for the conformational picture of **3** (Fig. 3). Two conformers (**4**_{Min1} and **4**_{Min2}) appeared to be important for conformational description of **4** (Fig. 4). Finally, two rotamers (**5**_{Min1} and **5**_{Min2}) were found significant for the description of **5** (Fig 5).

Thermodynamic data of **1**, **2**, **3**, **4**, and **5** were calculated at *HF* (6-31G*, 6-311G**), *B3LYP* (6-31G*, 6-311G**), and single point *MP2* (6-31G*, 6-311G**) level and are shown in Table 1. Included are: relative energies (E_r), enthalpies (H_r), and *Gibbs* free energies (G_r). All six levels of theory showed **1**_{Min3} to have smaller E_r , H_r , and G_r than those of all the conformers scrutinized. Hence, they were set at zero, while the E_r , H_r , and G_r of the other conformers were adjusted accordingly.

Table 1. Relative energies (E_r), enthalpies (H_r), and *Gibbs* free energies (G_r) for twenty-three conformers of the scrutinized tautomers **1–5** via *HF*, *B3LYP* and *MP2*. The global minimum, **1_{Min3}**, data (E_r , H_r , and G_r) are set at zero, while those of the other twenty-two conformers are adjusted accordingly

Conformers	Energies	<i>HF</i> /kJ mol ⁻¹		<i>B3LYP</i> /kJ mol ⁻¹		<i>MP2</i> /kJ mol ⁻¹	
		6-31G*	6-311G**	6-31G*	6-311G**	6-31G*	6-311G**
1_{Min1}	<i>E</i>	38.20	11.59	32.68	35.65		
	<i>H</i>	38.20	11.59	32.68	35.65	47.03	7.87
	<i>G</i>	35.02	10.54	29.46	32.22		
1_{Min2}	<i>E</i>	11.05	11.59	6.53	8.49		
	<i>H</i>	11.05	11.59	6.53	8.49	21.13	7.87
	<i>G</i>	10.71	10.54	6.53	8.03		
1_{Min3}	<i>E</i>	0.00	0.00	0.00	0.00		
	<i>H</i>	0.00	0.00	0.00	0.00	0.00	0.00
	<i>G</i>	0.00	0.00	0.00	0.00		
1_{Min4}	<i>E</i>	23.72	26.82	3.10	8.41		
	<i>H</i>	23.72	26.82	3.10	8.37	24.69	13.26
	<i>G</i>	24.31	27.28	4.81	10.33		
1_{Min5}	<i>E</i>	4.69	4.56	8.16	7.45		
	<i>H</i>	4.69	4.56	8.20	7.45	9.12	8.58
	<i>G</i>	3.64	3.72	6.49	6.40		
2_{Min1}	<i>E</i>	103.93	105.10	80.08	82.68		
	<i>H</i>	103.93	105.10	80.08	82.68	107.65	91.96
	<i>G</i>	104.77	105.39	82.59	84.89		
2_{Min2}	<i>E</i>	124.31	123.22	98.24	99.96		
	<i>H</i>	124.31	123.22	98.37	99.96	129.03	111.84
	<i>G</i>	124.98	123.76	99.75	101.42		
2_{Min3}	<i>E</i>	78.70	78.16	61.88	63.18		
	<i>H</i>	78.70	78.16	61.88	63.18	86.82	70.08
	<i>G</i>	79.58	78.32	64.48	65.31		
2_{Min4}	<i>E</i>	98.78	97.65	80.37	81.04		
	<i>H</i>	98.78	97.65	80.37	81.00	107.28	89.58
	<i>G</i>	99.54	98.07	82.55	83.30		
2_{Min5}	<i>E</i>	82.42	85.48	83.10	88.41		
	<i>H</i>	82.42	85.48	83.10	88.41	78.49	65.61
	<i>G</i>	84.89	87.78	84.81	89.33		
2_{Min6}	<i>E</i>	114.27	134.85	55.94	90.96		
	<i>H</i>	114.27	134.85	54.35	90.96	109.33	124.31
	<i>G</i>	117.19	134.85	57.95	91.50		
2_{Min7}	<i>E</i>	76.48	77.28	52.93	56.23		
	<i>H</i>	76.48	77.28	52.93	56.23	81.38	66.86
	<i>G</i>	76.99	76.69	55.69	58.87		
2_{Min8}	<i>E</i>	112.68	112.72	100.71	102.93		
	<i>H</i>	112.68	112.72	100.71	102.93	126.61	109.29
	<i>G</i>	109.58	109.04	101.25	103.09		
3_{Min1}	<i>E</i>	62.55	73.81	68.83	79.96		
	<i>H</i>	62.55	73.81	68.83	79.91	86.90	79.33
	<i>G</i>	58.32	69.66	64.98	76.23		
3_{Min2}	<i>E</i>	56.78	63.30	69.58	80.00		
	<i>H</i>	56.78	68.58	69.58	80.00	83.51	76.02
	<i>G</i>	52.72	64.22	63.72	76.23		

(continued)

Table 1 (continued)

Conformers	Energies	<i>HF</i> /kJ mol ⁻¹		<i>B3LYP</i> /kJ mol ⁻¹		<i>MP2</i> /kJ mol ⁻¹	
		6-31G*	6-311G**	6-31G*	6-311G**	6-31G*	6-311G**
3 _{Min3}	<i>E</i>	59.91	70.67	71.09	82.17		
	<i>H</i>	59.96	70.67	71.09	82.17	84.43	75.56
	<i>G</i>	55.98	67.24	66.53	78.20		
3 _{Min4}	<i>E</i>	61.88	74.18	71.76	84.06		
	<i>H</i>	61.88	74.18	71.76	84.06	84.35	79.50
	<i>G</i>	59.37	71.67	69.20	81.00		
3 _{Min5}	<i>E</i>	67.95	79.24	71.96	83.43		
	<i>H</i>	67.95	79.24	71.96	83.43	89.70	82.76
	<i>G</i>	64.60	76.32	68.37	79.91		
3 _{Min6}	<i>E</i>	65.06	77.40	73.43	87.99		
	<i>H</i>	65.06	77.40	75.77	87.99	88.41	82.89
	<i>G</i>	62.63	75.02	70.21	82.72		
4 _{Min1}	<i>E</i>	91.92	74.39	84.77	68.20		
	<i>H</i>	91.92	74.39	84.77	68.20	107.40	103.43
	<i>G</i>	91.13	74.06	84.22	66.57		
4 _{Min2}	<i>E</i>	78.32	62.55	64.73	49.62		
	<i>H</i>	78.32	62.55	64.73	49.62	83.43	52.80
	<i>G</i>	82.13	66.36	69.12	54.02		
5 _{Min1}	<i>E</i>	134.60	128.62	141.00	149.58		
	<i>H</i>	134.60	128.62	141.00	145.69	146.61	139.03
	<i>G</i>	134.14	127.99	139.62	165.64		
5 _{Min2}	<i>E</i>	142.55	137.15	147.07	143.05		
	<i>H</i>	142.55	137.15	147.07	143.05	144.68	137.86
	<i>G</i>	140.96	135.44	146.15	141.67		

A discrepancy was encountered between *HF*, *MP2* and *B3LYP* in calculating the global minimum for the conformers of **2**. On one hand, hydrogen bonding between oxygen and hydrogen (O–H–O) was observed in **2**_{Min5}, which was suggested by *MP2* methods (with 6-31G* and/or 6-311G** basis sets) to be the global minimum for conformers of **2**. The parameters involved in this hydrogen bonding were quite reasonable with the O–H distance of 0.960 Å and H–O distance of 1.746 Å, and with the corresponding ∠O–H–O motif angle of 106.1° (Fig. 2, Table 1). On the other hand, hydrogen bonding between nitrogen and hydrogen (O–H–N) was observed in **2**_{Min7}, which was suggested by the *HF* and *B3LYP* methods (with 6-31G* and/or 6-311G** basis sets) to be the global minimum for conformers of **2**. The parameters involved in this hydrogen bonding were also quite reasonable with an O–H distance of 0.954 Å and H–N distance of 2.111 Å, and with the corresponding ∠O–H–N motif angle of 111.2° (Fig. 2, Table 1).

Conversely, no discrepancy was encountered between *HF*, *MP2*, and *B3LYP* in calculating the global minima for conformers of **1**, **3**, **4**, or **5** tautomers. All the employed methods showed **1**_{Min3} to be the global minimum of **1** (Fig. 1, Table 1). Hydrogen bonding between oxygen and hydrogen (O–H–O) was observed in **1**_{Min4}. The parameters involved in this hydrogen bonding were: the O–H distance = 0.950 Å, H–O distance = 1.790 Å, and the corresponding ∠O–H–O motif angle = 142.4°. This conformer did not emerge as the global minimum of **1** due to the steric effects involved between its *ortho*-hydrogens and the β-CH₃ (Fig. 1, Table 1). Similarly, all the employed methods showed **4**_{Min2} to be the global minimum of **4** (Fig. 4, Table 1). Hydrogen bonding between oxygen and hydrogen (O–H–O) was observed in **4**_{Min2}. The parameters involved in this hydrogen bonding were: the O–H distance = 0.942 Å, H–O distance = 1.805 Å, and the corresponding ∠O–H–O motif angle = 114.5°. Finally, no hydrogen bonding was observed in any conformer of **3** and **5**; indicating

the higher significance of hydrogen bonding in stabilizing tautomers **2** and/or **4**. The lack of H-bonding in **3** and **5** was translated into the higher similarity between the energies of their corresponding rotamers (Table 1).

Free rotations around three single bonds (–) of **1**: *Ph*–C(NO)C(O)CH₃, *Ph*C(NO)–C(O)CH₃, and *Ph*C(N–OH)C(O)CH₃, gave five energy minima conformers (**1**_{Min1}, **1**_{Min2}, **1**_{Min3}, **1**_{Min4}, and **1**_{Min5}; Fig. 1). Similarly, rotations around three single bonds of **2**: *Ph*–C(NO)C(OH)CH₃, *Ph*C(N–O)C(OH)CH₃, and *Ph*C(NO)C(–OH)CH₃, gave eight structures (**2**_{Min1}, **2**_{Min2}, **2**_{Min3}, **2**_{Min4}, **2**_{Min5}, **2**_{Min6}, **2**_{Min7}, and **2**_{Min8}; Fig. 2) with no imaginary vibrational frequency. In the same manner, six minima (**3**_{Min1}, **3**_{Min2}, **3**_{Min3}, **3**_{Min4}, **3**_{Min5}, and **3**_{Min6}; Fig. 3) were found for **3** through rotations around *Ph*–CH(NO)C(O)CH₃, *Ph*CH(–NO)C(O)CH₃, and *Ph*CH(NO)–C(O)CH₃ bonds. Two minima (**4**_{Min1} and **4**_{Min2}) were found through rotations around four single bonds of **4**: *Ph*–C(NO)C(OH)CH₂, *Ph*C(N–OH)C(OH)CH₂, *Ph*C(NO)–C(OH)CH₂, and *Ph*–C(NO)C(–OH)CH₂ (Fig. 4). Similarly, two minima (**5**_{Min1} and **5**_{Min2}) were found through rotations around four single bonds of **5**: *Ph*–CH(NO)C(OH)CH₂, *Ph*CH(–NO)C(OH)CH₂, *Ph*CH(NO)–C(OH)CH₂, and *Ph*CH(NO)C(–OH)CH₂ (Fig. 5).

Interconversion pathways of the five conformers of **1** were probed through scanning (one and/or two dimensional), and/or QST3 (*B3LYP*/6-311G^{**}) techniques. The same treatments were adopted for the eight conformers of **2**, the six conformers of **3**, the two conformers of **4**, and the two conformers of **5**.

Rotations around single bonds rendered several conformers as minima for each tautomer. The lowest possible energy paths were selected for interconversion of these conformers. Two-dimensional scans were employed for the transition states not reachable through simple rotations around one bond. Search for a transition structure between (*E*) and (*Z*) conformers of **1** (and **2**) was carried out using the STQN (*B3LYP*/6-311G^{**}) method. This option required the input of the optimized reactand and product as well as proposed TS structures. Hence, the atoms were specified in the same order within the three structures (Figs. 1–5).

Different *ab initio* methods of calculations predicted unanimously that the global minimum of the oxime tautomer **1** is of the lowest energy compared

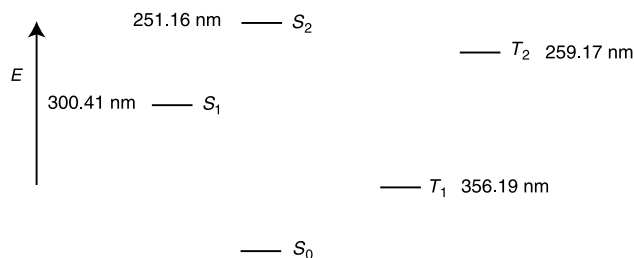


Fig. 6. Excited states energies (in the gas phase) and the multiplicities for **1** calculated at the CIS (6-311G^{**}) level of theory

to those of **2**, **3**, **4**, and **5**. In turn, the global minimum of **3** was found to be more stable than that of **2**. Hence, the order of the stability of global minima encountered was: **1** > **3** > **2** > **4** > **5**.

Gas phase, CIS/6-311G^{**} calculated, excited state *S*₁ appeared at: $\lambda_{\text{max}} = 300.4$ nm (Fig. 6), which was energetically slightly higher than the experimental value: $\lambda_{\text{max}} = 312.0$ nm (Fig. 7). The experimentally observed red shift of $\pi - \pi^*$ absorption of **1** is due to the bathochromic effect of the solvent (acetonitrile) [19].

The calculated IR spectra of **1** and its tautomers were compared with the experimental (Nujol mull, KBr plates) spectrum (Table 2 and Fig. 8). IR band assignments were done only on the major absorptions for the global minimum **1**_{Min3}, which was the most stable conformer of the most stable tautomer encountered (Table 2). The calculated normal mode

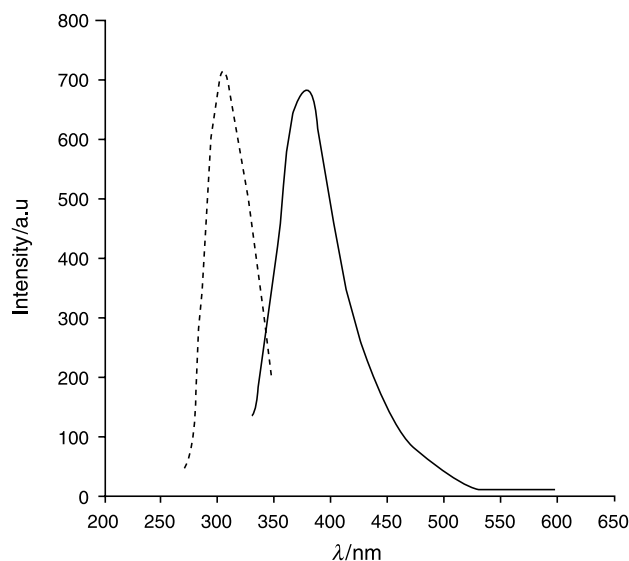


Fig. 7. Excitation and emission spectra for a $3 \cdot 10^{-3}$ M solution of **1** in acetonitrile at 25°C, $\lambda_{\text{ex}} = 312$ nm; $\lambda_{\text{em}} = 380$ nm

Table 2. Experimental and *B3LYP/6-311G*** calculated frequencies and IR intensities of the global minimum $\mathbf{1}_{\text{Min3}}$, which is the most stable conformer of the most stable tautomer encountered. Assignments are done only on the major absorptions. A scale factor of 0.9613 is applied to all *B3LYP/6-311G*** calculated frequencies

Normal mode	Theoretical		Experimental frequencies cm ⁻¹	Assignments
	Un-scaled frequencies cm ⁻¹	Scaled frequencies cm ⁻¹		
ν_{19}	707.63	680.24	680.0	Out of plane bending of C–H aromatic
ν_{27}	1006.02	967.09	953.6	Stretching N–O
ν_{39}	1387.72	1334.02	1349.2	Bending O–H
ν_{40}	1388.84	1335.09	1350.4	Bending C–H methyl
ν_{47}	1672.37	1607.65	1647.6	Stretching C=N oxime
ν_{48}	1771.98	1703.40	1652.2	Stretching C=O
ν_{49}	3049.96	2931.93	2910.1	Symmetric stretching C–H methyl
ν_{50}	3112.39	2991.94	2915.3	Asymmetric stretching C–H methyl
ν_{54}	3186.90	3063.57	3050.9	Stretching C–H aromatic
ν_{57}	3818.27	3670.50	3217.0	Stretching O–H

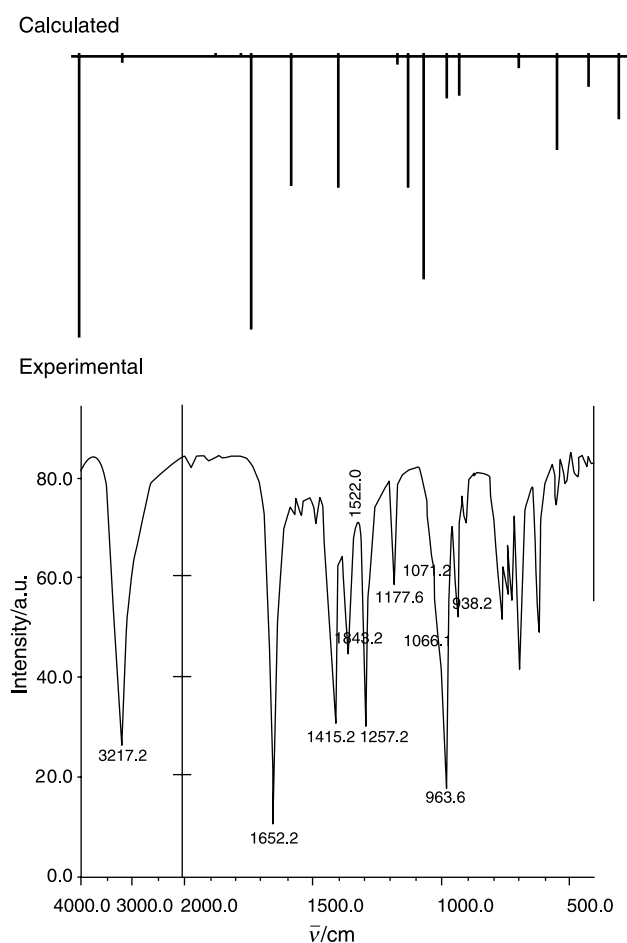


Fig. 8. Experimental (Nujol mull, KBr plates), and *B3LYP/6-311G*** calculated IR spectra of $\mathbf{1}_{\text{Min3}}$ as the most stable structural minimum encountered

27, at 967.09 cm⁻¹, might correspond to the experimental N–O stretching of the oxime at 953.6 cm⁻¹. Similarly, the calculated normal mode 47, at 1607.65 cm⁻¹, might correspond to the experimental C=N stretching of the oxime at 1647.6 cm⁻¹. Matching of the *B3LYP* calculated vibrational absorptions of $\mathbf{1}_{\text{Min3}}$ with those obtained experimentally suggested $\mathbf{1}_{\text{Min3}}$ as the structure of the oxime in the real world. Moreover, the observed band at 3670 cm⁻¹ could be attributable to the stretching mode of an (hydrogen bond free) OH group (Fig. 1).

A linear relationship was observed between the experimental and the scaled theoretical frequencies

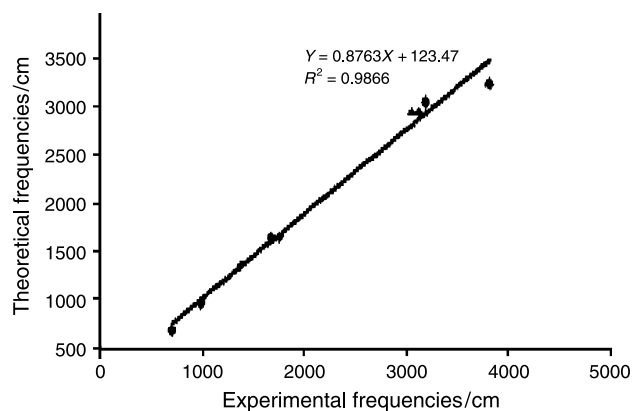


Fig. 9. Linear relationship applying a least square method is obtained. Correlation coefficient between experimental (Nujol mull, KBr plates) and theoretical (*B3LYP/6-311G***) vibration modes shows good agreement ($R = 0.993$) between the two methods

through the employment of the least square method (Fig. 9). The correlation coefficient (R^2) between experimental and theoretical vibration modes showed good agreement between the experimental and the scaled theoretical frequencies.

Conclusion

Ab initio calculations portrayed a clear picture of **1** and its tautomers **2–5**. The order of the stability of global minima encountered was found to be **1** > **3** > **2** > **4** > **5**. Hydrogen bonding was observed in two conformers of **2**, one of which turned out to be the global minimum; one conformer of **4**, which happens to be the global minimum; one conformer of **1**, which does not emerge as the global minimum; and no conformer of **3** and **5** indicating the higher significance of hydrogen bonding in tautomers **2** and **4**. Interconversion pathways of the five conformers of **1** were probed through scanning (one and/or two dimensional), and/or QST3 techniques. The same treatments are adopted for the eight conformers of **2**, the six conformers of **3**, the two conformers of **4**, and the two conformers of **5**.

Methods

Rotational energy profile around all the single bonds of **1**, **2**, **3**, **4**, and **5** (Figs. 1–5), were determined using *ab initio* HF calculation and STO-3G basis-sets. Calculations were performed by means of the Gaussian 98 system of programs [20]. Several optimizations were carried out for **1**, **2**, **3**, **4**, and **5**, each at a constant dihedral angle starting from 0° to 360° with 10° increments. All the other structural parameters were allowed to vary and be optimized. The geometrical structures, corresponding to the ground states and transition states were investigated at HF/STO-3G level of theory. To assess the performance of this approach, all species were computed at higher levels. Consequently, the STO-3G outputs were used as inputs for the HF/6-31G* calculations and the HF/6-31G* outputs were inputted for HF/6-31G**. The *Hartree–Fock* method usually works well for frequency predictions and geometry optimizations, but its utility for calculating conformational energy is questionable [21]. Hence, the necessity of investigating the effects of the electron correlations on the order of the magnitude of relative energies of the conformers arises. So, further post *Hartree–Fock* (MP2) single point calculations were performed on optimized geometries obtained through HF/6-31G* and HF/6-311G** [22]. Finally, the geometry reoptimizations were carried out using the DFT in the form of Becke's three parameters functional hybrid method [23]. This was with the Lee, Yang, and Parr correlation functional ((B3LYP)/6-31G*) and (B3LYP)/6-311G**) [24].

Transition state geometries were investigated by means of the QST3 technique. In each case, two optimized conformers along with their speculated transition state were used as input. In order to confirm the nature of the stationary species and evaluate the rotational activation energy barriers around each bond, frequency calculations (using the keyword: FREQ) were carried out for ground and transition states at both HF and DFT levels. The energy values were corrected with zero point vibrational energy to eliminate known systematic errors in calculations. All structures appeared to correspond to local minima, since frequency calculations yield only positive values at the equilibrium geometries. Structures were considered to be true transition states by having only one imaginary frequency. Also reaction path was followed by IRC to confirm transition states related to the corresponding minima [25, 26].

The fluorescence spectrum of **1** was recorded on a Perkin-Elmer LS-30 luminescence spectrometer equipped with a Xe lamp with acetonitrile as the solvent. Excited states energies and their multiplicities were contrasted with the calculated values obtained *via* the CIS option of Gaussian 98. Calculated and experimental IR spectra (Nujol mull, KBr plates) of **1** and its tautomers were compared.

Acknowledgements

This paper is dedicated to our beloved colleague Mr. A. Karimian, who rests in peace at this time; but without his sincere assistance this work would not have materialized.

References

- [1] Kolandaivel P, Senthilkumar K (2001) *J Mol Struct* **535**: 61
- [2] Kuze N, Suzuki E, Siratani M, Amako T, Okuda T, Kondo G, Kuriyama T, Matsubayashi M, Sakaizumi T, Ohashi O (1998) *J Mol Spect* **191**: 1
- [3] Buraway A, Cais M, Chamberlain J, Liversedge F, Thomson AR (1955) *J Chem Soc* 3727
- [4] Shpinel Y, Tarnopol'skii Y (1977) *Org Khim* **13**: 1030
- [5] Encheva V, Ivanovaa G, Stoyanov N (2003) *J Mol Struct (Theochem)* **640**: 149
- [6] Jaffe H (1955) *J Am Chem Soc* **77**: 4448
- [7] Krzan A, Crist D, Horak V (2000) *J Mol Struct (Theochem)* **528**: 237
- [8] Encheva V, Ivanovaa G, Ugrinova, Neykov G (1999) *J Mol Struct* **508**: 149
- [9] Ramalingama M, Venuvanalingam P, Swaminathanc J, Buemi G (2004) *J Mol Struct (Theochem)* **712**: 175
- [10] Verdoorn T, Johansen T, Drejer J, Nielsen E (1994) *Eur J Pharmacol* **269**: 43
- [11] Krzan A, Crist D, Horaçk V (2000) *J Mol Struct (Theochem)* **528**: 237
- [12] Burawoy A, Cais M, Chamberlain J, Liversedge F, Thompson A (1955) *J Chem Soc* 3721
- [13] Hadzi D (1956) *J Chem Soc* 2725
- [14] Iijima K, Ohashi O (1993) *J Mol Struct* **291**: 159
- [15] Iijima K, Matsuoka K, Sakaisumi T, Ohashi O (1996) *Bull Chem Soc Jpn* **69**: 2486

- [16] Kolandaivel P, Senthilkumar K (2001) *J Mol Struct (Theochem)* **535**: 61
- [17] Ren R, Ou W (2001) *Tet Lett* **42**: 8445
- [18] (a) Enchev V, Ivanova G, Ugrinov A, Neykov G (1999) *J Mol Struct* **508**: 149; (b) Enchev V, Ivanova G, Ugrinov A, Neykov G, Minchev S, Stoyanov N (1998) *J Mol Struct* **440**: 227
- [19] Aragoni M, Arca M, Demartin F, Devillanova F, Isaia F, Ggarau A, Lipolis V, Jalali F, Papke U, Shamsipur M, Tei L, Yari A, Verani G (2002) *Inorg Chem* **41**: 6623
- [20] GAUSSIAN 98, Revision A. 6, Frisch M, Trucks G, Schlegel H, Scuseria G, Robb M, Cheeseman J, Znkzrewski V, Montgomery G, Startmann R, Burant J, Dapprich S, Millam J, Daniels A, Kudin K, Strain M, Farkas O, Tomasi J, Barone V, Cossi M, Cammi R, Mennucci B, Pamelli C, Adamo G, Clifford S, Ochterski J, Petersson G, Ayala P, Cui Q, Morokoma K, Malick D, Rubuck A, Raghavachari K, Foresman J, Cioslawski J, Ortiz J, Stlefanov B, Liu G, Liashenko A, Piskorz P, Komaromi I, Comperts R, Martin R, Fox P, Keith T, Al-laham M, Peng C, Akkara A, Gonzales C, Combe M, Gill P, Johnson B, Chem W, Wong M, Andres J, Gonzales C, Head-Gordon M, Replogle E, Pople J (1998) Gaussian Inc., Pittsburgh, PA
- [21] Foresman J, Frisch E (1999) *Exploring chemistry with Electronic Structure Methods*, 2nd edn, Gaussian, Inc. Carnegie Office Park, Building 6, Pittsburgh, PA 15106, USA
- [22] Hehre W, Radom L, Schleyer P, Pople J (1986) *Ab initio Molecular Orbital Theory*. Wiley, New York
- [23] (a) Becke A, (1988) *Phys Rev A* **38**: 3098; (b) Becke A (1993) *J Chem Phys* **98**: 5648; (c) Parr R, Yang W (1989) *Density Functional Theory of Atoms and Molecules*; Oxford: New York (d) Ziegler T (1991) *Chem Rev* **91**: 651; (e) Lee C, Yang W, Parr R (1988) *Phys Rev B* **37**: 785; (f) For a description of density functionals as implemented in the Gaussian Series of programs, see: Johnson B, Gill P, Pople J (1993) *J Chem Phys* **98**: 5612
- [24] Hohenberg P, Kohn W (1964) *Phys Rev B* **136**: 864
- [25] Gonzalez C, Schlegel H (1989) *J Chem Phys* **90**: 2154
- [26] Gonzalez C, Schlegel H (1990) *J Chem Phys* **94**: 5523